

Thiolato–Technetium Complexes. Part 6.¹ Synthesis, Characterization, Electrochemical Properties and Crystal Structure of $[\text{Tc}(\text{tdt})(\text{dmpe})_2]\text{PF}_6$ [tdt = toluene-3,4-dithiolate, dmpe = 1,2-bis(dimethylphosphino)ethane] †

Takumi Konno,^a Jon R. Kirchhoff,^a Mary Jane Heeg,^{*,b} William R. Heineman^a and Edward Deutsch^{*,‡,a}

^a Biomedical Chemistry Research Center, Department of Chemistry, University of Cincinnati, Cincinnati, OH 45221-0172, USA

^b Department of Chemistry, Wayne State University, Detroit, MI 48202-3929, USA

The technetium(v) complex $[\text{Tc}(\text{OH})\text{O}(\text{dmpe})_2]^{2+}$ can be reduced by excess of toluene-3,4-dithiol (H_2tdt) to yield the technetium(III) complex $[\text{Tc}(\text{tdt})(\text{dmpe})_2]\text{PF}_6$. The product has been characterized by elemental analysis, UV/VIS spectroscopy, fast atom bombardment mass spectrometry and X-ray crystallography. It crystallizes in the triclinic space group $P\bar{1}$ with $Z = 2$, $a = 9.1508(9)$, $b = 12.794(2)$, $c = 13.516(2)$ Å, $\alpha = 93.94(1)$, $\beta = 95.24(1)$ and $\gamma = 108.791(9)^\circ$. The final R value was 0.037. The technetium co-ordination geometry is midway between octahedral and trigonal prismatic. Relevant structural parameters are Tc–S 2.318(6), S–C 1.738(4) Å, S–Tc–S bite angle $84.49(4)^\circ$ and Tc–P 2.402(7) Å. The entire tdt ligand is planar. Electrochemical and spectroelectrochemical measurements have been made for the reversible $\text{Tc}^{\text{III}}\text{--Tc}^{\text{II}}$ and $\text{Tc}^{\text{II}}\text{--Tc}^{\text{I}}$ couples at -0.600 and -1.217 V respectively vs. Ag–AgCl (3 mol dm^{-3} NaCl). A quasi-reversible $\text{Tc}^{\text{IV}}\text{--Tc}^{\text{III}}$ couple was observed at $+0.680$ V. The properties of $[\text{Tc}(\text{tdt})(\text{dmpe})_2]\text{PF}_6$ are compared to those observed previously for related *cis*- and *trans*- $[\text{Tc}(\text{SR})_2(\text{dmpe})_2]^{+/0}$ (R = alkyl or aryl) complexes.

The reactions of technetium with dithiols has been shown to generate a number of well characterized complexes.^{2–4} For the most part, they comprise square-pyramidal five-co-ordinate technetium(v) complexes $[\text{TcO}(\text{S–S})_2]^-$ where S–S is either an alkane- or arene-dithiolate ligand.^{5–8} Less prominent are those compounds which lack the $[\text{Tc}=\text{O}]^{3+}$ core. These are typically six-co-ordinate tris(chelate) complexes of ligands such as benzene-1,2-dithiolate (bdt) or toluene-3,4-dithiolate (tdt); $[\text{Tc}(\text{bdt})_3]^-$ and $[\text{Tc}(\text{tdt})_3]$, in which the technetium centre is formally in the +v and +vi oxidation states respectively, have been reported.^{9,10} Recently, the synthesis and structure of a technetium(IV) dithiolato complex, $[\text{Tc}_2(\text{bdt})_4]$, has appeared; this is a metal–metal bound dimer.^{11,12} Arene-1,2-dithiolate ligands characteristically^{13–15} stabilize the relatively unusual trigonal-prismatic geometry and structural analyses of both $[\text{Tc}(\text{bdt})_3]^-$ and $[\text{Tc}_2(\text{bdt})_4]$ have confirmed such co-ordination.¹⁶ Presumably $[\text{Tc}(\text{tdt})_3]$ is likewise trigonal prismatic although an X-ray structural analysis has not yet appeared.¹⁰

Technetium diphosphine complexes generally are low valent and octahedral, e.g. $[\text{Tc}(\text{dmpe})_3]^+$,^{17,18} where dmpe is 1,2-bis(dimethylphosphino)ethane and the technetium centre is in the +I oxidation state. The mixed-ligand complex $[\text{Tc}(\text{tdt})(\text{dmpe})_2]^+$ can be viewed as intermediate in composition between $[\text{Tc}(\text{dmpe})_3]^+$ and $[\text{Tc}(\text{bdt})_3]^-$. One goal of our study was to examine the structural properties of $[\text{Tc}(\text{tdt})(\text{dmpe})_2]^+$ to see if these would also be intermediate. In addition we sought to determine the redox properties of $[\text{Tc}(\text{tdt})(\text{dmpe})_2]^+$; since

this complex is isolated as Tc^{III} we inferred that its redox properties might be roughly intermediate to those of $[\text{Tc}(\text{dmpe})_3]^+$, which is isolated as Tc^{I} , and $[\text{Tc}(\text{tdt})_3]$, which is isolated as Tc^{VI} .

Our involvement with technetium dithiolato complexes stems from previous experience with the reactions of phosphinotechnetium complexes with monodentate thiols.^{1,19} This paper is the sixth in a series dealing with the synthesis and characterization of various $[\text{Tc}(\text{SR})_2(\text{dmpe})_2]^{+/0}$ complexes; these papers specifically report the fast atom bombardment (FAB) mass spectra, UV/VIS spectra, crystallography and accessible redox potentials of the various complexes under identical conditions in order to allow comparison of the effects generated by subtle changes in the R group of the thiol moiety. However, in studying the redox behaviour of these complexes, it is difficult to exclude the possibility of concurrent *cis/trans* isomerism along with electron transfer. By synthesising the chelating dithiolato derivative reported herein we have ensured that the redox chemistry occurs solely within the *cis* geometry. This redox chemistry can then be compared to that of the dihalogeno complexes $[\text{TcX}_2(\text{dmpe})_2]^{+/0}$ wherein the *trans* geometry is ensured by isolation and characterization of both the technetium-(II) and -(III) complexes in the *trans* form. The previously studied monodentate thiolato complex,¹⁴ *cis*- $[\text{Tc}(\text{SPh})_2(\text{dmpe})_2]^+$, also provides a natural basis for comparison to the present complex. Ultimately, the purpose of these studies is the development of novel technetium radiopharmaceuticals²⁰ through a better understanding of technetium chemistry.

Results and Discussion

Synthesis and Characterization.—A technetium(III) complex with a toluene-3,4-dithiolato ligand has been prepared: $[\text{Tc}(\text{tdt})(\text{dmpe})_2]^+$ was made by reduction of, and substitution onto, the technetium(v) complex $[\text{Tc}(\text{OH})\text{O}(\text{dmpe})_2]^{2+}$ by a

† Supplementary data available: see Instructions for Authors, *J. Chem. Soc., Dalton Trans.*, 1992, Issue 1, pp. xx–xxv.

Non-SI units employed: eV $\approx 1.60 \times 10^{-19}$ J; in = 2.54×10^{-2} m.

‡ Present address: Mallinckrodt Medical Inc., 675 McDonnell Blvd., P.O. Box 5840, St. Louis, MO 63134, USA.

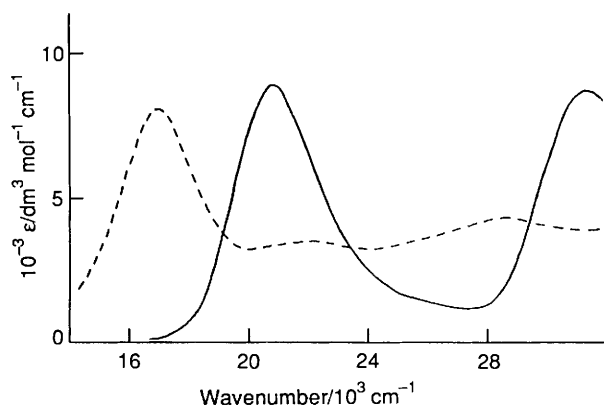


Fig. 1 The visible region absorption spectra of $[\text{Tc}(\text{tdt})(\text{dmpe})_2]^+$ (—) and $\text{cis}-[\text{Tc}(\text{SPh})_2(\text{dmpe})_2]^+$ (---) recorded in MeCN

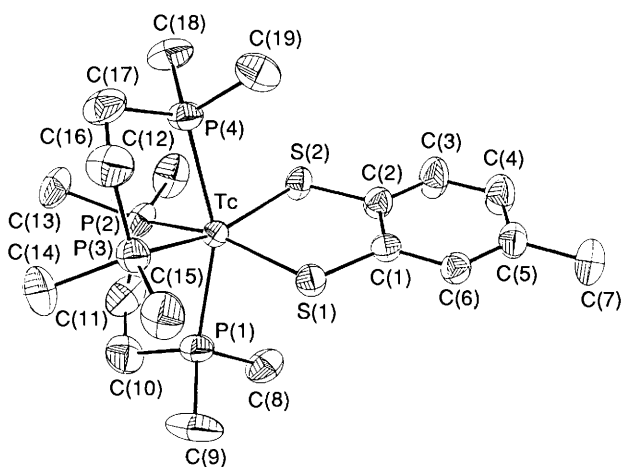


Fig. 2 A drawing of $[\text{Tc}(\text{tdt})(\text{dmpe})_2]^+$ with ellipsoids representing 50% probability and showing the assigned labelling

five-fold excess of toluene-3,4-dithiol. The reaction was initiated and enhanced by the addition of a small amount of base and it proceeded directly to the orange technetium(III) product. It was as fast as comparable reactions of $[\text{Tc}(\text{OH})\text{O}(\text{dmpe})_2]^{2+}$ with monodentate arenethiols^{1d} under the same conditions.

Simple ligand-substitution reactions have successfully generated many complexes of Tc^{V} and Tc^{IV} , often starting from an oxotechnetium(V) halide anion, $[\text{TcOX}_4]^-$, or a hexahalo-technetium(IV) dianion, $[\text{TcX}_6]^{2-}$.^{6,7,21,22} Lower oxidation states of Tc, viz. Tc^{III} and Tc^{II} , are more efficiently generated by reduction/substitution reactions, although these sometimes yield a variety of products in different oxidation states. This problem can be minimized by utilizing a starting material in which the oxidation state is lower than that in pertechnetate. We have had a good deal of success with $[\text{Tc}^{\text{V}}(\text{OH})\text{O}(\text{dmpe})_2]^{2+}$ as a starting material for the synthesis of a series of compounds of the form $[\text{Tc}(\text{SR})_2(\text{dmpe})_2]^{+0,1}$ in these reactions an excess of thiol acts as the reducing agent, presumably being oxidized to disulfide. The present work demonstrates the further usefulness of this synthetic route in the preparation of dithiolato complexes. The reduction/substitution reaction with a dithiolate proceeds under conditions exactly analogous to those employed for monodentate thiols. The product generated by monodentate HSR reduction is $[\text{Tc}^{\text{II}}(\text{SR})_2(\text{dmpe})_2]$; the corresponding technetium(III) complexes can be obtained by subsequent oxidation. However, in the dithiolato case, a technetium(III) complex, $[\text{Tc}(\text{tdt})(\text{dmpe})_2]^+$, is initially formed and there is no evidence of the technetium(II) species despite the use of an excess of dithiol. This is due largely to the fact that the $\text{Tc}^{\text{III}}-\text{Tc}^{\text{II}}$ redox potential is significantly more negative for $[\text{Tc}(\text{tdt})(\text{dmpe})_2]^+$ than for $\text{cis}-[\text{Tc}(\text{SR})_2(\text{dmpe})_2]^+$.^{1d}

Since the starting complex $[\text{Tc}(\text{OH})\text{O}(\text{dmpe})_2]^{2+}$ is in a *trans* geometry, rearrangement of the dmpe ligands occurs during the reaction with toluene-3,4-dithiol to generate a product with *cis* geometry. The same rearrangement is observed during the reaction of *trans*- $[\text{Tc}(\text{OH})\text{O}(\text{dmpe})_2]^{2+}$ with monodentate arenethiols, wherein the *cis* isomers, $\text{cis}-[\text{Tc}(\text{SC}_6\text{H}_4\text{-X-}p)_2(\text{dmpe})_2]^+$, are formed.^{1c,d} Similar reactions with alkanethiols maintain the geometry of the starting complex and only *trans* products are obtained.^{1a,b} It is clear that the arene group has an important role in the formation of a *cis* geometry. This role has been ascribed to the more demanding steric requirements of arenethiols relative to primary alkanethiols.^{1d,e}

The positive-ion FAB mass spectrum of $[\text{Tc}(\text{tdt})(\text{dmpe})_2]^+$ shows a single peak representative of the parent ion. No fragment due to loss of dithiolate or dmpe ligand is observed. For the corresponding bis(monodentate thiolato) complexes^{1a-d} both $\text{cis}-[\text{Tc}(\text{SC}_6\text{H}_4\text{X-}p)_2(\text{dmpe})_2]^+$ and $\text{trans}-[\text{Tc}(\text{SR})_2(\text{dmpe})_2]^+$ show fragment ions arising from the loss of one thiolate ligand. The tenacity of the Tc-S bonds in $[\text{Tc}(\text{tdt})(\text{dmpe})_2]^+$ during the mass spectroscopy experiment can be attributed to the chelate effect. Fragment ions due to the loss of a dmpe ligand have been commonly observed^{1d} for $\text{cis}-[\text{Tc}(\text{SC}_6\text{H}_4\text{X-}p)_2(\text{dmpe})_2]^+$ complexes, presumably due to the weakening of the Tc-P bond as a consequence of the thiolato structural *trans* effect (STE). The present dithiolato complex, $[\text{Tc}(\text{tdt})(\text{dmpe})_2]^+$ does not show the fragment ion resulting from the loss of a dmpe ligand, which is consistent with the lack of a significant STE in the crystal structure analysis.

Fig. 1 contrasts the visible spectra of $[\text{Tc}(\text{tdt})(\text{dmpe})_2]^+$ and $\text{cis}-[\text{Tc}(\text{SPh})_2(\text{dmpe})_2]^+$. The latter spectrum (dotted line) is typical of $\text{cis}-[\text{Tc}(\text{SR})_2(\text{dmpe})_2]^+$ (R = aryl) octahedral complexes with monodentate thiolate ligands, viz. there is an intense peak at 16 000–17 000 cm^{-1} accompanied by two less-intense peaks at ca. 22 000 and 29 000 cm^{-1} .^{1d} All three visible absorptions have been attributed to S→Tc charge-transfer bands. The spectrum of the related dithiolato complex $[\text{Tc}(\text{tdt})(\text{dmpe})_2]^+$ (solid line in Fig. 1) exhibits its lowest-energy peak at 20 800 cm^{-1} , which is 3800 wavenumbers higher in energy than the analogous band in $\text{cis}-[\text{Tc}(\text{SPh})_2(\text{dmpe})_2]^+$. Other visible transitions are likewise shifted to higher energies relative to those for $\text{cis}-[\text{Tc}(\text{SPh})_2(\text{dmpe})_2]^+$. Thus, the technetium centre in $[\text{Tc}(\text{tdt})(\text{dmpe})_2]^+$ is not as expected for Tc^{III} , but rather the energy of the S→Tc charge-transfer transitions are shifted towards those observed in complexes containing a technetium(II) centre. This and further observations (see below) indicate that the present complex behaves as if the technetium oxidation state were somewhat less than +III. The P→Tc charge-transfer bands expected to occur in the UV region are masked by the very intense ($\epsilon \approx 3.8 \times 10^4 \text{ dm}^3 \text{ mol}^{-1} \text{ cm}^{-1}$) absorption at 228 nm which corresponds to $\pi \rightarrow \pi^*$ transitions centred in the aromatic portion of the dithiolate ligand. Similar high-intensity UV transitions have been observed for $\text{cis}-[\text{Tc}(\text{SR})_2(\text{dmpe})_2]^+$ (R = aryl)^{1d} complexes but not for $\text{trans}-[\text{Tc}(\text{SR})_2(\text{dmpe})_2]^+$ (R = alkyl).^{1b}

Structure of $[\text{Tc}(\text{tdt})(\text{dmpe})_2]\text{PF}_6$.—Fig. 2 illustrates the molecular geometry and labelling scheme for the cation. Fractional atomic coordinates are listed in Table 1, selected bond lengths and angles in Table 2. All atoms occupy general positions in the unit cell. The ligand arrangement around Tc is intermediate between octahedral and trigonal prismatic. In perfect octahedral geometry the two *fac* planes are staggered creating a twist angle (θ) of 60° between the two triangular faces. Acute bite angles in chelated ligands result in lower twist angles as representative of their closest approach to octahedral geometry. Based on steric considerations alone, Kepert¹³ calculates minimum-energy conformations resulting in a 'best' twist angle of ca. 45° for bidentate chelates having 79° bite angles (as observed here for dmpe) and θ ca. 52° for 84° bite angles (as in the dithiolate ligand). When these two triangular planes are eclipsed, the twist angle is 0° representing a trigonal

Table 1 Fractional atomic parameters for $[\text{Tc}(\text{tdt})(\text{dmpe})_2]\text{PF}_6$

Atom	x	y	z
Tc	0.150 29(4)	0.224 66(3)	0.314 25(3)
S(1)	0.255 1(1)	0.238 44(9)	0.479 59(8)
S(2)	-0.020 9(1)	0.302 1(1)	0.379 84(8)
P(1)	0.395 3(1)	0.360 2(1)	0.295 8(1)
P(2)	0.093 1(2)	0.282 9(1)	0.153 84(9)
P(3)	0.262 6(1)	0.083 5(1)	0.273 30(9)
P(4)	-0.079 5(1)	0.067 3(1)	0.267 80(9)
P(5)	0.577 9(2)	0.257 2(1)	0.893 6(1)
C(1)	0.148 8(5)	0.295 3(3)	0.553 8(3)
C(2)	0.021 9(5)	0.321 4(4)	0.509 2(3)
C(3)	-0.066 9(6)	0.362 2(5)	0.569 3(4)
C(4)	-0.029 1(6)	0.378 4(5)	0.672 3(4)
C(5)	0.100 3(6)	0.356 0(4)	0.717 6(3)
C(6)	0.188 2(5)	0.315 1(4)	0.659 0(3)
C(7)	0.140 7(7)	0.377 4(5)	0.829 9(4)
C(8)	0.399 3(6)	0.490 0(4)	0.360 9(4)
C(9)	0.585 3(6)	0.354 1(5)	0.343 1(6)
C(10)	0.412 0(7)	0.391 1(4)	0.167 4(4)
C(11)	0.257 2(8)	0.398 0(5)	0.123 2(4)
C(12)	-0.062 7(8)	0.344 8(5)	0.138 6(4)
C(13)	0.048 9(7)	0.187 2(4)	0.038 6(4)
C(14)	0.353 6(7)	0.081 5(5)	0.159 0(4)
C(15)	0.404 8(7)	0.059 6(5)	0.364 6(4)
C(16)	0.111 7(7)	-0.055 3(4)	0.257 6(5)
C(17)	-0.038 3(6)	-0.048 9(4)	0.204 5(4)
C(18)	-0.254 2(6)	0.072 4(5)	0.195 8(5)
C(19)	-0.156 3(7)	0.010 5(5)	0.379 4(5)
F(1)	0.549 5(7)	0.166 0(4)	0.803 3(4)
F(2)	0.749 3(5)	0.311 7(5)	0.879 5(5)
F(3)	0.617 4(9)	0.178 4(5)	0.961 9(5)
F(4)	0.608 6(7)	0.342 8(5)	0.984 0(4)
F(5)	0.406 7(5)	0.200 5(5)	0.912 3(5)
F(6)	0.538 7(9)	0.332 3(4)	0.823 2(5)

Table 2 Selected bond lengths (Å) and angles (°) for $[\text{Tc}(\text{tdt})(\text{dmpe})_2]\text{PF}_6$

Tc-S(1)	2.322(1)	Tc-P(4)	2.393(1)
Tc-S(2)	2.313(1)	S(1)-C(1)	1.737(4)
Tc-P(1)	2.399(1)	S(2)-C(2)	1.739(4)
Tc-P(2)	2.408(1)	C(1)-C(2)	1.404(6)
Tc-P(3)	2.406(1)		
Tc-S(1)-C(1)	108.1(1)	S(1)-Tc-P(2)	158.70(3)
Tc-S(2)-C(2)	108.3(1)	S(1)-Tc-P(3)	89.46(3)
P(1)-Tc-P(2)	78.83(4)	S(1)-Tc-P(4)	113.68(4)
P(1)-Tc-P(3)	87.90(4)	S(1)-C(1)-C(2)	119.6(3)
P(1)-Tc-P(4)	157.41(4)	S(2)-Tc-P(1)	112.92(4)
P(2)-Tc-P(3)	102.96(3)	S(2)-Tc-P(2)	89.86(4)
P(2)-Tc-P(4)	85.91(4)	S(2)-Tc-P(3)	157.53(4)
P(3)-Tc-P(4)	79.35(4)	S(2)-Tc-P(4)	83.32(4)
S(1)-Tc-S(2)	84.49(4)	S(2)-C(2)-C(1)	119.4(3)
S(1)-Tc-P(1)	84.48(4)		

prism. In $[\text{Tc}(\text{tdt})(\text{dmpe})_2]^+$ the mean twist angle is $33(3)^\circ$, nearly midway between the ideal forms. The *trans* bonding angles also make the geometry apparent. Here, S-Tc-P and P-Tc-P *trans* angles average $157.9(7)^\circ$, midway between expected values for the trigonal-prism (ca. 136°) and trigonal-antiprism (ca. 180°), but this value is often ca. 175° due to the distortion resulting from the bite angles) arrangements.

1,2-Dithiolate ligands are known for their ability to stabilize the relatively unusual trigonal-prismatic co-ordination geometry.¹³⁻¹⁵ Nearly all trigonal-prismatic metal complexes have been formulated with ligands containing sulfur or selenium donor atoms.^{13,23} Since this geometry is attained at the expense of normal ligand-ligand steric repulsions, it has been postulated¹⁵ that some type of interligand S...S bonding interaction is operating to distort these complexes from the more usual and sterically favoured octahedral geometry.

The mixed-ligand complex $[\text{Tc}(\text{tdt})(\text{dmpe})_2]^+$ is intermediate between the two limiting geometries, octahedral and trigonal prismatic. The dmpe ligand generally forms octahedral complexes and $[\text{Tc}(\text{dmpe})_3]^+$ is as octahedral as possible within the constraints of the dmpe bite angle.¹⁸ Therefore the trigonal-prism distortion of $[\text{Tc}(\text{tdt})(\text{dmpe})_2]^+$ has been introduced by the dithiolate ligand. The oxidation state of technetium (+3) is relatively low compared to those of the majority of trigonal-prismatic complexes. Eisenberg¹⁵ has theorized that highly oxidized metal ions better accommodate trigonal-prismatic geometry since they leave little electron density localized on the sulfur donor atoms, which in turn minimize electronic repulsions in the S...S contact. Acting in the opposite direction, dmpe stabilizes low metal oxidation states by M→L back bonding and the $[\text{Tc}(\text{dmpe})_3]^+$ complex is isolated as Tc^{I} .¹⁷

The complex $[\text{Tc}(\text{bdt})_3]^-$ has been structurally characterized⁹ and provides a good comparison to $[\text{Tc}(\text{tdt})(\text{dmpe})_2]^+$. The former has 'near-perfect' trigonal-prismatic co-ordination; the S-Tc-S bite angle (81.8°) and the S...S intrachelate distance (3.06 Å) are both smaller than those of the present complex [$84.49(4)^\circ$ and $3.116(2)$ Å], consistent with its co-ordination geometry. However, the mean Tc^V-S distance in $[\text{Tc}(\text{bdt})_3]^-$ is $2.336(5)$ Å compared to the Tc^{III}-S length of $2.318(5)$ Å in $[\text{Tc}(\text{tdt})(\text{dmpe})_2]^+$. It is expected that Tc^V-S would be shorter than Tc^{III}-S (due to the difference in ionic radii) if sulfur acts primarily as a σ-donor ligand. Since this is not the case here it suggests that π bonding may be of some importance in technetium dithiolate complexes. The Tc-S length in $[\text{Tc}(\text{tdt})(\text{dmpe})_2]^+$ fits nicely into the range observed for five-co-ordinate $[\text{Tc}^{\text{V}}\text{O}(\text{L})_2]^-$ (L = dithiolate) complexes (2.30-2.32 Å),⁵⁻⁸ which contain Tc in the +v oxidation state but also contain the strong π-donor oxide ligand. Also, five-co-ordinate complexes display M-L lengths somewhat lower than analogous six-co-ordinate complexes in this class.³

We have previously shown¹⁴ that, for a series of similar octahedral dmpe-thiol-technetium complexes, the Tc^{III}-S bond lengths are 2.29-2.30 Å while the Tc^{II}-S lengths are 2.42 Å. These distances are remarkably constant and dependent only on technetium oxidation state. On this basis the mean Tc^{III}-S distance in $[\text{Tc}(\text{tdt})(\text{dmpe})_2]^+$ (2.32 Å) is slightly long for a technetium(III)-thiol length, again implying some technetium(II) character in the formally technetium(III) centre.

The S-Tc-S bite angle in $[\text{Tc}(\text{tdt})(\text{dmpe})_2]^+$, $84.49(4)^\circ$, is larger than observed in most tris(1,2-dithiolato)metal complexes (ca. $80-82^\circ$)^{9,24-31} and is closer in value to that of five-co-ordinate $[\text{TcO}(\text{L})_2]^-$ (L = dithiolate) complexes ($84.7-85.2^\circ$).⁵⁻⁸ The S-C distance in $[\text{Tc}(\text{tdt})(\text{dmpe})_2]^+$ [$1.738(4)$ Å] is similar to that of tris(dithiolato) complexes^{9,24} but is considerably shorter than that in $[\text{Tc}(\text{SR})_2(\text{dmpe})_2]^{+/0}$ (R = aryl) complexes (ca. 1.77 Å).¹⁴ This is generally taken to imply some multiple-bond character in the S-C bond in 1,2-dithiolate ligands. The entire tdt ligand in $[\text{Tc}(\text{tdt})(\text{dmpe})_2]^+$ is planar to 0.03 Å and Tc is included in this plane. Both planar and bent examples of dithiolate ligands have been reported.⁹

The Tc-P bonds in other *cis*-bis(dmpe) technetium thiolato complexes exhibit a shorter length *trans* to phosphorus than *trans* to sulfur.^{1c,d} However the Tc-P lengths here average $2.396(3)$ Å *trans* to P and $2.407(1)$ Å *trans* to S, yielding a calculated structural *trans* influence of only 0.011 Å. Because the crystallographic estimated standard deviations (e.s.d.s) reflect precision rather than accuracy, we agree with Glusker and Trueblood³² that '... it is usually unwise to regard measured interatomic distances in crystals as more accurate than to the nearest 0.01 Å'. Therefore all four Tc-P bond lengths in $[\text{Tc}(\text{tdt})(\text{dmpe})_2]^+$ are nearly equivalent and little or no structural *trans* influence is observed.

A number of structural determinations of six-co-ordinate technetium thiol dmpe complexes¹⁴ have yielded average Tc-P bond distances. For $[\text{Tc}(\text{SR})_2(\text{dmpe})_2]^{+/0}$, Tc^{III}-P averages $2.427(9)$ Å when P is *trans* to P. The Tc^{II}-P mean distance is

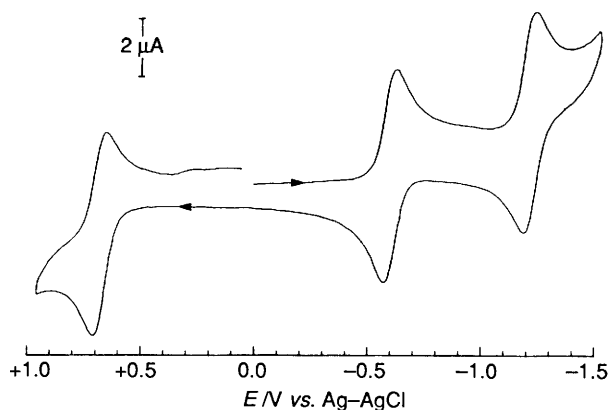


Fig. 3 Cyclic voltammogram of $0.97 \text{ mmol dm}^{-3} [\text{Tc}(\text{tdt})(\text{dmpe})_2]\text{PF}_6$ in $0.5 \text{ mol dm}^{-3} \text{NEt}_4\text{ClO}_4$ -dmf at a platinum disk electrode at room temperature. Scan rate 100 mV s^{-1}

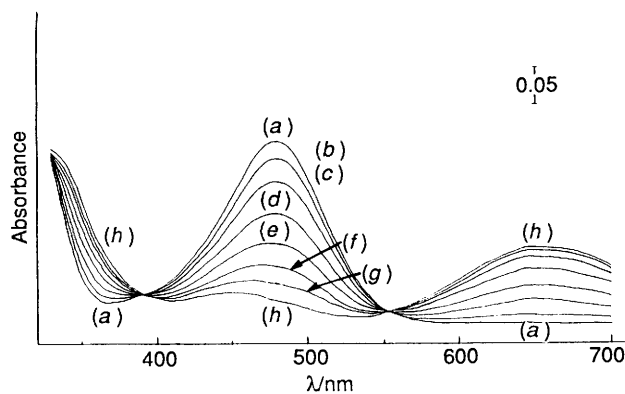


Fig. 4 Absorption spectra recorded during the potentiostatic reduction of $1.12 \text{ mmol dm}^{-3} [\text{Tc}(\text{tdt})(\text{dmpe})_2]\text{PF}_6$ in $0.5 \text{ mol dm}^{-3} \text{NEt}_4\text{ClO}_4$ -dmf in the optically transparent thin-layer electrode. Applied potentials in V vs. Ag-AgCl are as follows: (a) 0.0; (b) -0.51; (c) -0.54; (d) -0.56; (e) -0.58; (f) -0.60; (g) -0.62; (h) -0.90

$2.391(8) \text{ \AA}$ when P is *trans* to P. Both Tc-P distances are longer when S is the *trans* ligand. In the present structure $\text{Tc}^{\text{III}}\text{-P}$ is $2.402(7) \text{ \AA}$. This is significantly shorter than expected for $\text{Tc}^{\text{III}}\text{-P}$ and much nearer the $\text{Tc}^{\text{II}}\text{-P}$ expected value. Technetium-phosphorus bond lengths decrease with decreasing technetium oxidation state in these complexes due to the increasing importance of Tc→P π -back bonding. In another summary,^{1a} Tc-P bond distances have been tabulated for diverse six-coordinate technetium complexes and mean values are $\text{Tc}^{\text{I}}\text{-P}$ $2.39(3)$ (range 2.34–2.43), $\text{Tc}^{\text{II}}\text{-P}$ $2.43(2)$ (range 2.41–2.45), $\text{Tc}^{\text{III}}\text{-P}$ $2.46(3)$ (range 2.42–2.52) and $\text{Tc}^{\text{IV}}\text{-P}$ $2.49(2)$ (range 2.47–2.53 \AA). It is obvious that the Tc-P lengths in $[\text{Tc}(\text{tdt})(\text{dmpe})_2]^+$ are relatively short, resembling those of technetium(II) complexes; thus, once again the technetium centre acts as if its oxidation state were between Tc^{III} and Tc^{II} . This is consistent with the relatively high-energy visible S→Tc charge-transfer bands (see above) and the more negative E° ($\text{Tc}^{\text{III}}\text{-Tc}^{\text{II}}$) potential (see below) compared to those of other $[\text{Tc}(\text{SR})_2(\text{dmpe})_2]^+$ (R = aryl) complexes.

There are other perturbations within the structure of $[\text{Tc}(\text{tdt})(\text{dmpe})_2]^+$ that are apparently a result of the trigonal-prismatic distortion. The octahedral complexes *cis*- $[\text{Tc}^{\text{II}}(\text{SC}_6\text{H}_4\text{Cl-}i>p)_2(\text{dmpe})_2]$ and *cis*- $[\text{Tc}^{\text{III}}(\text{SPh})_2(\text{dmpe})_2]^+$ exhibit thiol-induced STEs of 0.05 and 0.07 \AA respectively.^{1d} Chemical evidence presented thus far in this report has shown that the toluenedithiolate ligand is an effective σ donor, however the difference between *cis* and *trans* Tc-P bond lengths in $[\text{Tc}(\text{tdt})(\text{dmpe})_2]^+$ is barely significant. The dilution of the STE is certainly associated here with the trigonal-prism distortion. The P-Tc-P dmpe bite angle in $[\text{Tc}(\text{tdt})(\text{dmpe})_2]^+$ is the

smallest recorded for $[\text{Tc}(\text{SR})_2(\text{dmpe})_2]^{+/0}$ complexes^{1a,c,d} [$79.1(3)$ vs. a range of $80.5(2)$ – $82.5(1)^\circ$], also consistent with the tendency toward trigonal-prismatic geometry.

Very recently the synthesis and structure of $[\text{Tc}^{\text{III}}(\text{OC}_6\text{H}_4\text{-SH-}o)(\text{dmpe})_2]^+$ has been published,³³ where the ligand is analogous to tdt except that it possesses S,O rather than S,S donor atoms. The trigonal-prismatic distortion from octahedral geometry in $[\text{Tc}(\text{OC}_6\text{H}_4\text{SH-}o)(\text{dmpe})_2]^+$ is clear, although it is to a lesser extent than in $[\text{Tc}(\text{tdt})(\text{dmpe})_2]^+$. The average twist angle is $36(2)^\circ$. The average Tc-P distance [$2.38(3) \text{ \AA}$] is shorter than those observed in comparable technetium(III) dmpe complexes. Further structural comparisons to $[\text{Tc}(\text{OC}_6\text{H}_4\text{SH-}o)(\text{dmpe})_2]^+$ are fruitless due to disorder in the ligand, but these observations support our conclusion: in these trigonally distorted complexes, the $\text{Tc}^{\text{III}}\text{-P}$ length is more comparable to that of a lower technetium oxidation state.

The atoms of the PF_6 anion exhibit large thermal parameters but not unusually so. The P-F distances average $1.53(3) \text{ \AA}$ and F-P-F (*cis*) angles are in the range 86.0 – 94.1° .

Electrochemistry.—Fig. 3 illustrates the cyclic voltammogram at a platinum disk electrode for a $0.97 \text{ mmol dm}^{-3}$ solution of $[\text{Tc}(\text{tdt})(\text{dmpe})_2]^+$ in $0.5 \text{ mol dm}^{-3} \text{NEt}_4\text{ClO}_4$ -dimethylformamide (dmf). A negative potential scan initiated at 0.0 V reveals two sequential reduction waves with peak potentials of -0.630 and -1.245 V . Upon reversing the scan at -1.55 V the corresponding reoxidation waves are observed at -1.189 and -0.570 V . In accordance with the previously reported electrochemistry of technetium(III) thiolato complexes,^{1b,d,e} these two redox processes are assigned as $\text{Tc}^{\text{III}}\text{-Tc}^{\text{II}}$ and $\text{Tc}^{\text{II}}\text{-Tc}^{\text{I}}$ reversible redox couples with E° values of -0.600 and -1.217 V , respectively. The reversibility of both redox couples is established by the criteria set forth in previous papers of this series. Continuation of the positive potential scan reveals the oxidation of Tc^{III} to Tc^{IV} with a peak potential of $+0.711 \text{ V}$ and the associated reduction of Tc^{IV} to Tc^{III} at $+0.649 \text{ V}$ ($E^\circ = +0.680 \text{ V}$). However the observations that (i) the ratio of i_{pc}/i_{pa} is 0.6:1 and (ii) several small peaks appear between -0.3 and 0.0 V indicate that the $\text{Tc}^{\text{IV}}\text{-Tc}^{\text{III}}$ redox couple is not chemically reversible.

The spectra recorded during the spectropotentiostatic reduction of $[\text{Tc}(\text{tdt})(\text{dmpe})_2]^+$ in $0.5 \text{ mol dm}^{-3} \text{NEt}_4\text{ClO}_4$ -dmf are shown in Fig. 4. The technetium(III) complex has an absorption maximum at 479 nm , whereas the technetium(II) complex exhibits maxima at 646 , 452 and a shoulder at 338 nm . Isoestic points are maintained at 552 and 390 nm . A Nernst plot^{34–36} of the data at 479 nm yields $E^\circ = -0.566 \text{ V}$ and $n = 1.00$.

The electrochemistry of the $[\text{Tc}(\text{tdt})(\text{dmpe})_2]^+$ complex is similar to that observed for the $[\text{Tc}(\text{SR})_2(\text{dmpe})_2]^+$ complexes,^{1b,d,e} yet with some distinctive features of its own. A unique feature of the system is the fact that three redox couples are observed at room temperature, *i.e.* two reversible one-electron reductions ($\text{Tc}^{\text{III}}\text{-Tc}^{\text{II}}$ and $\text{Tc}^{\text{II}}\text{-Tc}^{\text{I}}$) and a quasi-reversible one-electron oxidation ($\text{Tc}^{\text{III}}\text{-Tc}^{\text{IV}}$). Contrariwise, several previously reported monodentate thiolato complexes exhibit the quasi-reversible $\text{Tc}^{\text{III}}\text{-Tc}^{\text{IV}}$ couple only at -70°C .^{1b,d,e} Furthermore, the $\text{Tc}^{\text{III}}\text{-Tc}^{\text{II}}$ E° value of -0.600 V for $[\text{Tc}(\text{tdt})(\text{dmpe})_2]^+$ indicates that this complex is one of the hardest technetium(III) thiolates to reduce. This stabilization of the oxidation states Tc^{III} and Tc^{IV} for $[\text{Tc}(\text{tdt})(\text{dmpe})_2]^+$ is clearly a result of the influence of the bidentate tdt ligand.

Values of E° of this magnitude have been observed for the $\text{Tc}^{\text{III}}\text{-Tc}^{\text{II}}$ redox couple of technetium(III) alkanethiolato complexes where the strong σ -donor properties of the SR ligand stabilize Tc^{III} and thus inhibit reduction of Tc^{III} to Tc^{II} .^{1b} For complexes wherein enhanced π -acid character is introduced to the ligand either as pendant substituents^{1b,d} or as part of the ligand backbone^{1c} as is the case for tdt, E° generally shifts to potentials more positive than those of the technetium(III) alkanethiolato complexes. Therefore it may be reasonable

to attribute the unusually negative $Tc^{III}-Tc^{II}$ E° value of $[Tc(tdt)(dmpe)_2]^+$ to an effect other than simple ligand donor properties. One possibility is that the change in molecular symmetry caused by the trigonal-prismatic distortion raises the absolute energy of the redox-active molecular orbital and counteracts the opposing effect engendered by the π -acid character of $[Tc(tdt)(dmpe)_2]^+$.

The absorption spectra recorded during the spectropotentiostatic reduction of $[Tc^{III}(tdt)(dmpe)_2]^+$ [spectrum (a), Fig. 4] to $[Tc^{II}(tdt)(dmpe)_2]$ [spectrum (h), Fig. 4] demonstrate spectral changes similar to those described for the *cis*- $[Tc(SR)_2(dmpe)_2]^{+/0}$ (R = aryl) complexes¹⁴ in that the predominant visible peak of the technetium(III) species is absent for the reduced species. The position of the S→Tc charge-transfer absorption maximum of Tc^{III} is influenced by the geometry induced by the tdt ligand. The most intense visible band occurs at an energy higher than for all previously reported thiolato dmpe complexes of Tc^{III} , i.e. 479 nm for $[Tc(tdt)(dmpe)_2]^+$ vs. 588–599 nm for *cis*- $[Tc(SR)_2(dmpe)_2]^+$ (R = aryl) and 596–611 nm for *trans*- $[Tc(SR)_2(dmpe)_2]^+$ (R = alkyl). This band of $[Tc(tdt)(dmpe)_2]^+$ is higher in energy than even that for comparable technetium(II) complexes: *cis*- $[Tc(SR)_2(dmpe)_2]$ (R = aryl) (510–536 nm)¹⁴ and *trans*- $[Tc(SR)_2(dmpe)_2]$ (R = alkyl) (536–542 nm).^{1b}

The quality of robustness is important in the design of radiopharmaceuticals which must resist *in vivo* reactions. The complex $[Tc(dmpe)_3]^+$ is non-reducible *in vivo*³⁷ but presents only limited possibilities for the introduction and manipulation of pendant substituents to control its biological distribution. The dichloro complex $[TcCl_2(dmpe)_2]^+$ has demonstrated *in vivo* reduction³⁷ with measured $E^\circ(Tc^{III}-Tc^{II}) = -0.231$ V vs Ag–AgCl,³⁸ and the dibromo congener is even easier to reduce with $E^\circ(Tc^{III}-Tc^{II}) = -0.098$ V vs. Ag–AgCl.³⁸ Substitution of alkanethiolate ligands for the halides enhances the stability of Tc^{III} , e.g. $[Tc(SMe)_2(dmpe)_2]^+$ has $E^\circ(Tc^{III}-Tc^{II}) = -0.550$ V vs. Ag–AgCl.^{1b} However somewhat less of a gain in stability is achieved with arenethiolate ligands, e.g. $[Tc(SPh)_2(dmpe)_2]^+$ has $E^\circ(Tc^{III}-Tc^{II}) = -0.299$ V vs Ag–AgCl.¹⁴ Another potentially undesirable aspect of these monodentate thiolato complexes is that there can be accompanying *cis*–*trans* isomerization that produces a mixture of products. The present complex is suitably robust in that no such isomerization can occur. Further it has successfully incorporated an arenethiolate ligand without concomitant lowering of the reduction potential into the biologically accessible range. Viewed from another perspective, the complex demonstrates that introduction of dmpe ligands onto $[Tc(tdt)_3]$ imparts a structural and electrochemical stability lacking in $[Tc(tdt)_3]$, which undergoes a one-electron reduction at $E^\circ = +0.18$ V (vs. saturated calomel electrode) with apparent dimerization or polymerization.¹⁰

Conclusion

Careful comparison of the chemical properties of $[Tc(tdt)(dmpe)_2]^+$ with those of $[Tc(SR)_2(dmpe)_2]^{+/0}$ (R = aryl or alkyl) demonstrates the following. (i) For $[Tc(tdt)(dmpe)_2]^+$ the visible energy S→Tc charge-transfer bands appear at higher energy than predicted. (ii) The Tc–S length is slightly longer than expected while Tc–P is shorter than expected. (iii) The $Tc^{III}-Tc^{II}$ reduction potential is unusually negative for the class of arenethiolato complexes. All together these observations suggest a lower effective nuclear charge on Tc than in similar octahedral complexes. That is, the trigonal-prismatic distortion within $[Tc(tdt)(dmpe)_2]^+$ is accompanied by some degree of 'technetium(II) character' in the chemical characteristics of the technetium centre.

Experimental

CAUTION: Technetium-99 emits a low-energy (0.292 MeV) β particle with a half-life of 2.12×10^5 y. When handled in milligram amounts, it does not present a serious health hazard

since common laboratory materials provide adequate shielding. *Bremsstrahlung* is not a significant problem due to the low energy of the emission, but normal radiation safety procedures must be used at all times, especially when dealing with solid samples, to prevent contamination and inadvertent inhalation. In this paper the symbol Tc refers only to technetium-99; the metastable isotope ^{99m}Tc was not used.

Reagents.—Unless otherwise noted, all chemicals were of reagent grade. The starting complex, *trans*- $[Tc(OH)O(dmpe)_2][PF_6]_2$, was prepared as described previously.^{1a} The magic bullet matrix [dithiothreitol–dithioerythritol (5:1) in a small amount of methanol] was used in the measurement of the FAB mass spectrum. Dimethylformamide from Burdick and Jackson and polarographic grade NET_4ClO_4 from G. F. Smith Chemicals were used in the electrochemical measurements; prior to use, the latter was dried at 60 °C *in vacuo* over P_2O_5 . No significant electroactive impurities were detected in either the solvent or supporting electrolyte.

Synthesis.— $[Tc(tdt)(dmpe)_2]PF_6$. To a solution containing *trans*- $[Tc(OH)O(dmpe)_2][PF_6]_2$ (100 mg, 2.1×10^{-4} mol) in degassed ethanol (20 cm³) was added neat tdt (0.15 cm³, 1.1×10^{-3} mol), followed by 1 mol dm⁻³ NaOH (0.5 cm³). The mixture was stirred at 60 °C for 20 min under an argon atmosphere while it turned deep orange. After addition of saturated NH_4PF_6 (0.3 cm³), the orange solution was cooled to room temperature and the dark orange crystalline product precipitated was filtered off. Yield: 60 mg (41%). Dark orange crystals for X-ray structural analysis were obtained by recrystallization of this product from acetone–ethanol (1:1) at room temperature (Found: C, 29.7; H, 5.8; P, 22.1; S, 9.7. Calc. for $C_{19}H_{38}F_6P_5S_2Tc$: C, 32.7; H, 5.5; P, 22.2; S, 9.2%). UV/VIS (MeCN): λ_{max} 481 (8.97), 398(sh) (1.67), 320 (8.87), 258(sh) (11.57) and 228 nm (ϵ 38.28 dm³ mol⁻¹ cm⁻¹). FAB mass spectrum (magic matrix): m/z 553 (M^+). Elemental analysis of this complex gave a poorer than expected result for carbon, due in part to the formation of carbides in the combustion process and the very small amount of this radioactive material available for analysis.

Measurements.—Elemental analysis was performed by Galbraith Laboratories, Knoxville, TN. The UV/VIS spectra were recorded in acetonitrile on a Cary 210 spectrophotometer (Varian) at ambient temperature. The FAB mass spectrum was recorded using the magic bullet matrix on a VG 30–250 spectrometer (VG Instruments) at the probe temperature. Xenon was used as the primary beam gas and the ion gun was operated at 8 keV and 100 μ A. Data were collected over the mass range 100–1000 at 0.7 s per scan. Electrochemical measurements were made with a Bioanalytical Systems (BAS) CV-1B voltammograph. Potentials were monitored with a Keithley 178 digital multimeter and voltammograms were recorded on a Hewlett-Packard 7015B X-Y recorder. The visible spectrum in the spectroelectrochemical experiment was also recorded on a Cary 210 spectrophotometer; the cell compartment was modified to accommodate electrical leads and an inert-gas inlet. The working electrode for conventional cyclic voltammetry was a platinum disk (BAS). Optically transparent thin-layer electrodes were constructed as previously described with 100 wires per inch gold minigrad.³⁴ An aqueous Ag–AgCl (3 mol dm⁻³ NaCl) electrode (BAS) and a platinum wire were used as reference and auxiliary electrodes, respectively. The reference electrode was isolated from the solution by a porous Vycor plug. All potentials are reported vs. the Ag–AgCl (3 mol dm⁻³ NaCl) electrode. In general electrochemical experiments were performed as previously described.^{1b,d,e,38,39} Each spectrum in the spectropotentiostatic experiments was recorded 5 min after potential application. This time was sufficient to attain equilibrium values of [oxidised species]/[reduced species] in dmf solution.

Table 3 Crystallographic data* for [Tc(tdt)(dmpe)₂]PF₆

Colour, habit	Dark purple rhomboids
Dimensions/mm	0.25 × 0.25 × 0.15
<i>M</i>	698.41
Space group	<i>P</i> $\bar{1}$ (no. 2)
<i>a</i> /Å	9.1508(9)
<i>b</i> /Å	12.794(2)
<i>c</i> /Å	13.516(2)
α /°	93.94(1)
β /°	95.24(1)
γ /°	108.791(9)
<i>U</i> /Å ³	1483.6(3)
<i>Z</i>	2
<i>D</i> _c /g cm ⁻³	1.563
μ /cm ⁻¹	9.20
<i>F</i> (000)	712
Scan method	θ-2θ
λ (Mo-K α)/Å	0.710 73 (monochromated)
Scan range	1.0° below K α ₁ to 1.0° above K α ₂
Scan rate/° min ⁻¹	2-5
Background/scan time	0.5
2θ range/°	5-52
<i>T</i> /°C	28
Maximum and minimum $\Delta\rho$ on final ΔF map/e Å ⁻³	+0.76 (near PF ₆), -0.48
Transmission coefficients	0.852-0.791
<i>hkl</i> ranges	0 ≤ <i>h</i> ≤ 12, -16 ≤ <i>k</i> ≤ 16, -17 ≤ <i>l</i> ≤ 17
Total data	6053
Unique data	5863
Observed data [<i>I</i> ≥ 3σ(<i>I</i>)]	4407
<i>R</i>	0.037
<i>R</i> '	0.047
Weight	(σ _{<i>F</i>} ² + 0.0004 <i>F</i> ²) ⁻¹

* *R* = (Σ|Δ*F*|)/Σ|*F*_o|; *R*' = [(Σ*w*|Δ*F*²)/Σ*wF*_o²]^{1/2}. Lattice constants were derived from 24 high-angle reflections.

Crystallography.—Single-crystal X-ray diffraction experiments were performed on a Nicolet R3 automated diffractometer. The structure was solved by Patterson methods and refined in a full matrix using the SHELX 76 programs.⁴⁰ All non-hydrogen atoms were refined anisotropically. Hydrogen atoms were placed in observed positions and held invariant. Isotropic thermal parameters for the hydrogen atoms were assigned to be equal and refined as a single variable. No correction for secondary extinction was made. Neutral atom scattering factors and corrections for anomalous dispersion were from ref. 41. Table 3 contains the abstracted crystallographic data.

Additional material available from the Cambridge Crystallographic Data Centre comprises H-atom coordinates, thermal parameters and remaining bond lengths and angles.

Acknowledgements

Financial support by the National Institute of Health (grant nos. HL-21276 and CA-42179 to E. D.), by the Department of Energy (grant DE-FG02-86ER60487 to W. R. H.) and by Mallinckrodt (to E. D.) is gratefully acknowledged. The diffractometer used was purchased through a National Science Foundation equipment grant to Wayne State University.

References

- (a) Part 1, T. Konno, M. J. Heeg and E. Deutsch, *Inorg. Chem.*, 1988, **27**, 4113; (b) Part 2, T. Konno, J. R. Kirchhoff, W. R. Heineman and E. Deutsch, *Inorg. Chem.*, 1989, **28**, 1174; (c) Part 3, T. Konno, M. J. Heeg and E. Deutsch, *Inorg. Chem.*, 1989, **28**, 1694; (d) Part 4, T. Konno, M. J. Heeg, R. Seeber, J. R. Kirchhoff, W. R. Heineman and E. Deutsch, *Transition Met. Chem.*, 1992, in the press; (e) Part 5, T. Konno, M. J. Heeg, J. A. Stuckey, J. R. Kirchhoff, W. R. Heineman and E. Deutsch, *Inorg. Chem.*, 1992, **31**, 1173.
- E. Deutsch, K. Libson, S. Jurisson and L. F. Lindoy, *Prog. Inorg. Chem.*, 1983, **30**, 75.

- G. Bandoli, U. Mazzi, E. Roncari and E. Deutsch, *Coord. Chem. Rev.*, 1982, **44**, 191.
- M. Melnik and J. E. Van Lier, *Coord. Chem. Rev.*, 1987, **77**, 275.
- S. F. Colmanet and M. F. Mackay, *Aust. J. Chem.*, 1988, **41**, 151.
- S. F. Colmanet and M. F. Mackay, *Aust. J. Chem.*, 1987, **40**, 1301.
- B. V. DePamphilis, A. G. Jones, M. A. Davis and A. Davison, *J. Am. Chem. Soc.*, 1978, **100**, 5570.
- J. E. Smith, E. F. Byrne, F. A. Cotton and J. C. Sekutowski, *J. Am. Chem. Soc.*, 1978, **100**, 5571.
- S. F. Colmanet, G. A. Williams and M. F. Mackay, *J. Chem. Soc., Dalton Trans.*, 1987, 2305.
- M. Kawashima, M. Koyama and T. Fujinaga, *J. Inorg. Nucl. Chem.*, 1976, **38**, 801.
- S. F. Colmanet and M. F. Mackay, *J. Chem. Soc., Chem. Commun.*, 1987, 705.
- S. F. Colmanet and M. F. Mackay, *Aust. J. Chem.*, 1988, **41**, 269.
- D. L. Kepert, *Inorganic Stereochemistry*, Springer, New York, 1982.
- P. J. Blower and J. R. Dilworth, *Coord. Chem. Rev.*, 1987, **76**, 121.
- R. Eisenberg, *Prog. Inorg. Chem.*, 1970, **12**, 295.
- J. Baldas, J. Boas, J. Bonnyman, M. F. Mackay and G. A. Williams, *Aust. J. Chem.*, 1982, **35**, 2413.
- J.-L. Vanderheyden, A. R. Ketring, K. Libson, M. J. Heeg, L. Roecker, P. Motz, R. Whittle, R. C. Elder and E. Deutsch, *Inorg. Chem.*, 1984, **23**, 3184.
- V. Subramanian, personal communication.
- U. Abram, R. Beyer, P. Mading, I. Hoffman, R. Münze and J. Stach, *Z. Anorg. Allg. Chem.*, 1989, **578**, 229; J. Stach, U. Abram and R. Münze, *Z. Chem.*, 1989, **29**, 249.
- E. Deutsch and K. Libson, *Comments Inorg. Chem.*, 1984, **3**, 83; M. J. Clarke and L. Podbielski, *Coord. Chem. Rev.*, 1987, **78**, 253; C. L. Jones, in *Comprehensive Coordination Chemistry*, eds. G. Wilkinson, R. D. Gillard and J. McCleverty, Pergamon, Oxford, 1987, vol. 6, pp. 881-1009; A. M. Verbruggen, *Eur. J. Nucl. Med.*, 1990, **17**, 346.
- M. E. Kastner, P. H. Fackler, M. J. Clarke and E. Deutsch, *Inorg. Chem.*, 1984, **23**, 4683.
- A. Davison and A. G. Jones, *Int. J. Appl. Radiat. Isot.*, 1982, **33**, 875.
- D. L. Kepert, *Prog. Inorg. Chem.*, 1977, **23**, 1.
- M. Cowie and M. J. Bennett, *Inorg. Chem.*, 1976, **15**, 1584.
- M. Cowie and M. J. Bennett, *Inorg. Chem.*, 1976, **15**, 1589.

- 26 M. Cowie and M. J. Bennett, *Inorg. Chem.*, 1976, **15**, 1595.
27 R. Eisenberg and J. A. Ibers, *Inorg. Chem.*, 1966, **5**, 411.
28 R. Eisenberg and H. B. Gray, *Inorg. Chem.*, 1967, **6**, 1844.
29 G. F. Brown and E. I. Stiefel, *Inorg. Chem.*, 1973, **12**, 2140.
30 J. L. Martin and J. Takats, *Inorg. Chem.*, 1975, **14**, 1358.
31 F. W. B. Einstein and R. D. G. Jones, *J. Chem. Soc. A*, 1971, 2762.
32 J. P. Glusker and K. N. Trueblood, *Crystal Structure Analysis A Primer*, 2nd edn., Oxford University Press, New York, 1985, p. 164.
33 R. Münze, U. Abram, J. Stach and W. Hiller, *Inorg. Chim. Acta*, 1991, **186**, 151.
34 T. P. DeAngelis and W. R. Heineman, *J. Chem. Educ.*, 1976, **53**, 594.
35 W. R. Heineman, *Denki Kagaku*, 1982, **50**, 142.
36 J. R. Kirchoff, W. R. Heineman and E. Deutsch, *J. Pharm. Biomed. Anal.*, 1986, **4**, 777.
37 E. Deutsch and W. Hirth, *J. Nucl. Med.*, 1987, **28**, 1491.
38 A. Ichimura, W. R. Heineman, J.-L. Vanderheyden and E. Deutsch, *Inorg. Chem.*, 1984, **23**, 1272.
39 D. F. Rohrbach, W. R. Heineman and E. Deutsch, *Inorg. Chem.*, 1979, **18**, 2536.
40 G. M. Sheldrick, SHELX 76, University Chemical Laboratory, Cambridge, 1976.
41 *International Tables for X-Ray Crystallography*, Kynoch Press, Birmingham, 1974, vol. 4 (present distributor D. Reidel, Dordrecht).

Received 12th May 1992; Paper 2/02459D